UC Irvine
UC Irvine Previously Published Works

Title

Controls on methane released through ebullition in peatlands affected by permafrost degradation

Permalink

https://escholarship.org/uc/item/7pk481z7

Journal

Journal of Geophysical Research Biogeosciences, 119(3)

ISSN

2169-8953

Authors

Klapstein, Sara J
Turetsky, Merritt R
McGuire, A David
et al.

Publication Date

2014-03-01

DOI

10.1002/2013jg002441

Copyright Information

Peer reviewed

Key Points:
- Total ebullition and was greatest depended on seasonal thaw and changes in atmospheric pressure
- Ebullition was dominated by episodic ebullition and was greatest in the youngest thaw site
- Up to 22% of methane in late season bubbles was derived from older permafrost carbon

Correspondence to:
S. J. Klapstein,
saraklapstein@gmail.com

Controls on methane released through ebullition in peatlands affected by permafrost degradation

Sara J. Klapstein[1], Merritt R. Turetsky[1], A. David McGuire[2], Jennifer W. Harden[3], Claudia I. Czimczik[4], Xiaomei Xu[4], Jeffrey P. Chanton[5], and James M. Waddington[6]

[1]Department of Integrative Biology, University of Guelph, Guelph, Ontario, Canada, [2]Alaska Cooperative Fish and Wildlife Research Unit, U.S. Geological Survey and University of Alaska Fairbanks, Fairbanks, Alaska, USA, [3]U.S. Geological Survey, Menlo Park, California, USA, [4]Department of Earth System Science, University of California, Irvine, California, USA, [5]Department of Earth, Ocean, and Atmospheric Science, Florida State University, Tallahassee, Florida, USA, [6]School of Geography and Earth Sciences, McMaster University, Hamilton, Ontario, Canada

Abstract Permafrost thaw in peat plateaus leads to the flooding of surface soils and the formation of collapse scar bogs, which have the potential to be large emitters of methane (CH_4) from surface peat as well as deeper, previously frozen, permafrost carbon (C). We used a network of bubble traps, permanently installed 20 cm and 60 cm beneath the moss surface, to examine controls on ebullition from three collapse bogs in interior Alaska. Overall, ebullition was dominated by episodic events that were associated with changes in atmospheric pressure, and ebullition was mainly a surface process regulated by both seasonal ice dynamics and plant phenology. The majority (>90%) of ebullition occurred in surface peat layers, with little bubble production in deeper peat. During periods of peak plant biomass, bubbles contained acetate-derived CH_4 dominated (>90%) by modern C fixed from the atmosphere following permafrost thaw. Post-senescence, the contribution of CH_4 derived from thawing permafrost C was more variable and accounted for up to 22% (on average 7%), in the most recently thawed site. Thus, the formation of thermokarst features resulting from permafrost thaw in peatlands stimulates ebullition and CH_4 release both by creating flooded surface conditions conducive to CH_4 production and bubbling as well as by exposing thawing permafrost C to mineralization.

1. Introduction

Understanding the source of methane (CH_4) emissions is important for assessing feedback between carbon (C) storage in northern wetlands and Earth's climate systems. Carbon rapidly cycling between plants and microbes has a near-zero effect on atmospheric C, while decomposition of older C, which was not part of the active C cycle for centuries to millennia, results in a net flux of C to the atmosphere [*Trumbore*, 2009]. As permafrost in northern ecosystems continues to thaw, more organic matter that was previously thermally and physically protected within permafrost will be available for mineralization [*Schuur et al.*, 2009]. In ice-rich permafrost, soil C post-thaw may be kept under saturated conditions and exposed to slower, less efficient anaerobic pathways of decomposition such as methanogenesis (reduction of acetate or CO_2 to CH_4) [*Wickland et al.*, 2006; *Harden et al.*, 2012]. Whether permafrost-derived C is emitted primarily as CH_4 or carbon dioxide (CO_2) is a key uncertainty for assessing permafrost C-climate feedback, because CH_4 has a warming potential 34 times that of CO_2 on a 100 year time scale [*Intergovernmental Panel on Climate Change*, 2013].

Assessing CH_4 emissions from northern wetlands is difficult, as wetlands are diverse and dynamic landscapes. For example, permafrost peatlands such as peat plateaus tend to have minimal CH_4 emissions, because of relatively dry surface soil in the active layer [*Turetsky et al.*, 2002]. Permafrost thaw and thermokarst convert peat plateaus into collapse scar bogs or fens, which can support high rates of CH_4 production and emission [*Turetsky et al.*, 2002; *Wickland et al.*, 2006; *Prater et al.*, 2007]. Previous studies have measured 10- to 30-fold increases in CH_4 emissions from collapse bogs relative to adjacent intact permafrost plateaus in Canada and interior Alaska [*Turetsky et al.*, 2002; *Wickland et al.*, 2006].

Production and transport of CH_4 through wetlands is affected by a variety of biotic and abiotic controls, such as substrate availability, vegetation density and type, temperature, water table depth, and redox potential.

Methanogenesis requires anaerobic conditions. Once produced, CH_4 can be transported through the soil column, where it is either converted to CO_2 by aerobic microbial methanotrophy, or released to the atmosphere [*Whalen*, 2005]. Diffusion of CH_4 tends to contribute little to CH_4 emissions in peatlands. Instead, the transport pathways that dominate CH_4 emissions usually include both plant-mediated passive gas transport and ebullition [*Blodau*, 2002]. These two mechanisms allow for a rapid movement of gas from the water table to the atmosphere, potentially bypassing the aerobic soil layer and limiting methanotrophy [*Chanton*, 2005; *Coulthard et al.*, 2009]. Several studies have focused on plant-mediated transport [*Chanton and Dacey*, 1991; *Schutz and Schroder*, 1991; *King et al.*, 1998; *Cronk and Fennessy*, 2001], but less is known about the controls on ebullition.

Ebullition occurs because CH_4 has low solubility in aqueous environments and therefore readily exsolves and forms gas bubbles [*Hutchinson*, 1957]. While recent field and lab studies have recognized the importance of ebullition to total CH_4 emissions from northern wetlands [*Rosenberry et al.*, 2003; *Baird et al.*, 2004; *Coulthard et al.*, 2009], there is uncertainty about where in the peat bubbles are formed, stored, and released. Bubbles have been found to form in deep, water-saturated peat [*Glaser et al.*, 2004]. However, other research suggests that CH_4 production and bubble formation occur primarily in surface peat, where plant exudates stimulate methanogenesis [*Baird et al.*, 2004; *Kellner et al.*, 2006; *Coulthard et al.*, 2009]. Because thermokarst in peat plateaus can lead to flooding, permafrost thaw in these systems has the potential to stimulate anaerobiosis and the production of bubbles from both thawing deep and flooded surface peat layers.

Here we explored the depth of bubble production in the peat column as well as the radiocarbon (^{14}C) signature of bubble C to learn more about the source of C contributing to ebullition in wetlands experiencing permafrost thaw. We hypothesized that if plant exudates drove ebullition, we would observe (1) a positive relationship between plant abundance and bubble production, (2) maximum ebullition rates occurring during peak plant biomass, (3) bubbles dominated by C recently fixed from atmospheric CO_2 with a modern ^{14}C signature, and (4) bubble production largely in near-surface peat near the rooting zone. However, if older C from thawing permafrost soils (i.e., the previously frozen C pool) contributed to ebullition, we predicted that (1) ebullition rates would increase in parallel with seasonal increases in soil temperatures and thaw depth, and (2) bubbles would be produced from older, ^{14}C-depleted C sources in deeper peat layers, particularly later in the growing season with increased thaw depth. In addition, we investigated physical and environmental controls on ebullition. Following previous studies [*Tokida et al.*, 2007; *Comas et al.*, 2011], we predicted that absolute changes in atmospheric pressure would be correlated with large rates of bubble production across all of our sites. We also predicted that there would be positive relationships between soil temperature, depth to seasonal ice, and bubble production rates.

2. Study Sites

Research was conducted in the Alaska Peatland Experiment (APEX) sites (64.70°N, −148.32°W) located near the Bonanza Creek Experimental Forest on the Tanana Valley floodplain in interior Alaska, USA (http://www.lter.uaf.edu/). The climate is subarctic boreal with an average annual temperature of −2.9°C and 269 mm of precipitation [*Hinzman et al.*, 2005]. We studied three small ($<2000\,m^2$) collapse scar bogs that were located within a forested (*Picea mariana* black spruce) peat plateau and all within 30–40 m of each other. The ground surface of the collapse bogs has subsided by 0.5–1.0 m relative to the surrounding peat plateau where the active layer is approximately 40 cm deep. Our measurements took place between 16 June and 13 September 2011. Seasonal ice (i.e., ground ice that thaws each year during the growing season and refreezes each winter) was not present in the upper 30 cm of peat in our sites over the entire sampling period but was present in deeper peat layers at the start of the sampling campaign. Our sites are underlain by a talik zone, a region of ground that remains unfrozen all year round, and thus, the deepest peat in each site remains unfrozen year round.

Permafrost thaw histories at the three sites were reconstructed using vegetation reconstruction and ^{14}C dating of moss macrofossils from peat cores. At the "intermediate collapse" and the "old collapse" sites, the transition from permafrost peat at depth to post-thaw vegetation closer to the surface of peat cores occurred at approximately 28 and 82 cm, respectively. Radiocarbon dating of moss macrofossils manually picked from peat cores from both sites yielded a mean post-thaw peat accumulation rate of 0.22 ± 0.08 cm/yr

provided by M. C. Jones and J. W. Harden (unpublished data, 2014). This accumulation rate is similar to post-thaw dynamics in a neighboring collapse scar in the Tanana Valley floodplain [*Jones et al.*, 2012]. Thus, these data indicate that permafrost began to thaw at the intermediate collapse site around A.D. 1880 and at the old collapse site around A.D. 1640. At the "young collapse" site, the transition from permafrost peat at depth to post-thaw vegetation near the surface of peat cores occurred around 30 cm, but the results of radiocarbon dating of macrofossils were modern. Therefore, we suggest that the discrepancy between age and peat depth between the young collapse and the older thaw features is due to progressive compaction of loose surface peat that occurs in these sites over time. Here we make a conservative assumption that permafrost at the young collapse site began to thaw around A.D. 1910. Modern vegetation community structure in each site supports our interpretation of this thaw chronology. The young collapse site is dominated by *Sphagnum riparium*, *Carex aquatilis*, *Eriophorum chamissonis*, and *Eleocharis palustre* which often dominate collapse features soon after thaw. Although the intermediate collapse site has a similar species pool, there is more evidence of hummock formation and drier-adapted species such as *Sphagnum fuscum* than is present at the young collapse. Finally, there is more shrub colonization including *Andromeda polifolia*, *Chamaedaphne calyculata*, and *Ledum palustre* at the old collapse site, which is a normal component of autogenic succession following permafrost thaw [*Beilman*, 2001].

3. Methods

3.1. Environmental, Vegetation, and Peat Property Measurements

Surface peat in collapse scar bogs is extremely sensitive to disturbances, and therefore, all measurements included in this study were conducted from permanent raised boardwalks. We designed our boardwalks trying to minimize potential sampling disturbances by anchoring vertical support posts into mineral soils and surrounding vertical posts with smooth PVC piping to allow the peat to move with potential water table fluctuations.

At each site, we measured seasonal ice depth (distance from the moss surface to seasonally frozen soil) 1–3 times each week using a 1.5 m long metal rod in 6–8 locations per site. Soil temperature at 5 cm depth was measured hourly with thermistors connected to data loggers (Campbell Scientific, Logan, UT, USA); hourly measurements were averaged to determine daily means per site. Volumetric moisture content (%VMC; accurate to ±1%) within the top 5 cm of peat was measured 2–3 times per week using a ThetaProbe soil moisture sensor (Delta-T Devices, Cambridge, UK) inserted vertically into the surface peat. The ThetaProbe was calibrated in the lab using peat cores following the method outlined in *Kasischke et al.* [2009]. While the position of the water tables were recorded in each site hourly, water table fluctuations in our three collapse scar bogs were minimal. The water table remained close to the moss surface (within 5 cm) throughout the measurement period of this study. Since there was little variation in water table position, we did not include this variable as an environmental predictor of bubble accumulation rate. The APEX weather station, located approximately 1 km from the study sites, continuously measured atmospheric pressure using a Campbell CS100 Serta barometric pressure sensor (accuracy ±0.5 mbar). Because the sites were close together, barometric pressure was assumed to be comparable between sites.

Stem density for each vascular species was counted at peak biomass in 0.25 m^2 plots around each bubble trap (see bubble analysis methods section below) and scaled up to 1 m^2. Vascular plants were identified to species level and then sedges were grouped and analyzed as a single functional group, given that the three species found at our sites (*C. aquatilis*, *E. chamissonis*, and *E. palustris*) have been documented to be important for plant-mediated transport of CH_4 [*Shea*, 2010]. Percent cover of live moss was also determined in the 0.25 m^2 area surrounding each bubble trap.

Three soil cores (25 cm length and 5 cm diameter) were extracted from each site on 25 July 2011 to determine bulk and root density. Roots were hand sorted from one-half core, classified by size (fine roots <2 mm diameter; coarse roots ≥2 mm), and then dried and weighed to get root density (mg roots cm^{-3} core). To calculate bulk density, half the core was dried at 60°C to constant mass. Peat strength at the center of each site was determined on 1 August 2011 using a 1.5 m metal penetrometer rod [*Waddington et al.*, 2010], and a peat strength index was calculated for each site as the average number of hits required to lower the penetrometer through the peat column by 1 cm.

3.2. CH_4 Bubble Analysis

In each site, we installed bubble traps 20 cm below the moss surface. These traps captured all bubbles produced and transported in the peat column below 20 cm depth due to the buoyant nature of gas bubbles under water-saturated conditions. We installed the 20 cm bubble traps along boardwalks from the edge to the center of each collapse scar bog, which coincided with the location of our permanent boardwalks, resulting in $n = 10$ at the young collapse, $n = 7$ at the intermediate collapse, and $n = 8$ at the old collapse. Bubble traps were constructed using inverted plastic funnels connected to a 10 mL syringe via Tygon tubing and PVC using a method adapted from *Strack et al.* [2005], with a footprint area of 314 cm². During installation, a block of surface peat, the same size as the trap's funnel area, was carefully cut out by hand with a bread knife. The trap was then placed in the hole, and the peat core was cut in half and placed back around the PVC pipe to reestablish the peat layer on top of the funnel. Pore water was manually drawn up the funnel and into the syringe at the top of the trap above the peat surface at the beginning of the field season. Bubbles that then entered the funnel area moved up through the trap's water column and into the very top of the syringe, thereby displacing the syringe water downward.

Installation disturbance mostly involved surface peat and had minimal influence on deeper peat layers located underneath each trap. While we cannot rule out installation disturbance on our measurement of ebullition, two lines of evidence suggest that potential disturbance artifacts were minimal (1) extensive examination of hydrostatic pressure in peat carried out by *Kellner et al.* [2005] suggests that this trap design does not impact hydrostatic pressure, (2) comparison of bubble traps installed in 2011 during this study to bubble traps installed in 2009 showed no difference in bubble production rates ($p > 0.05$), suggesting that any impacts to surface peat or roots during installation did not affect bubble production and capture. Further, we note that all 20 cm bubble traps were installed in our three collapse bogs using the same methodology, and thus, any sampling artifacts would affect rates of bubble production across all traps.

Deeper 60 cm bubble traps were constructed similarly to the 20 cm traps but had longer PVC pipes and smaller funnels given that the bubble collection footprint was limited by the auger (Snow, Ice, and Permafrost Research Establishment corer) we used for installation through the seasonal ice. The footprint for the 60 cm bubble traps was 86.5 cm². Because these deeper cores were more difficult to extract from the collapse scar bogs, we were limited to installing only two 60 cm bubble traps in the center of each site. We relied on bootstrapping techniques (see section 3.4 below) to investigate whether the limited number of these 60 cm bubble traps influenced our results. While the 20 cm bubble traps captured the entire peat column bubble production (including below 60 cm), by examining the difference in bubble accumulation rates between the 20 cm and 60 cm bubble traps, we were able to assess the contribution of deeper (60+ cm) peat layers to bubble production.

Accumulation of gas within the syringe of each bubble trap was quantified visually every 1–4 days throughout the sampling period. All measurements were made from raised boardwalks. We did not observe bubbling to occur during these measurements, nor did our bubble traps register additional accumulation of bubbles after people accessed the boardwalks. Daily bubble production rates were calculated by dividing the total amount of bubble gas accumulated within each trap by the number of days between readings. This approach was effective for quantifying cumulative ebullition over the sampling period but may have dampened the magnitude of episodic ebullition events. When gas volumes >5 mL accumulated within each trap's syringe, the gas was extracted and analyzed for CH_4 concentration. Samples were analyzed within 24 h on a Varian 3900 gas chromatograph (GC) system equipped with a Haysep Q column and flame ionization detector (Varian Inc., Palo Alto, CA, USA) at the University of Alaska, Fairbanks. The GC was calibrated each day using external standards (0, 10.1, 100, 10,000, 100,000, and 500,000 ppm CH_4), which encompassed the full range of CH_4 concentrations measured in our samples.

3.3. Isotope Measurements and Analysis

To determine the source of bubble C, we measured the ^{14}C content of trapped bubbles using the bomb spike approach [*Trumbore*, 2006]. Aboveground nuclear weapon's testing during the 1950s and 1960s increased the amount of radioactive ^{14}C ($t_{1/2} = 5730$) in atmospheric CO_2 above natural production levels. After test cessation, the amount of bomb ^{14}C in the atmosphere has declined as a consequence of mixing with terrestrial and ocean C pools and emissions of fossil (^{14}C-free) fuel origin CO_2 [*Levin et al.*, 2010]. The mixing of
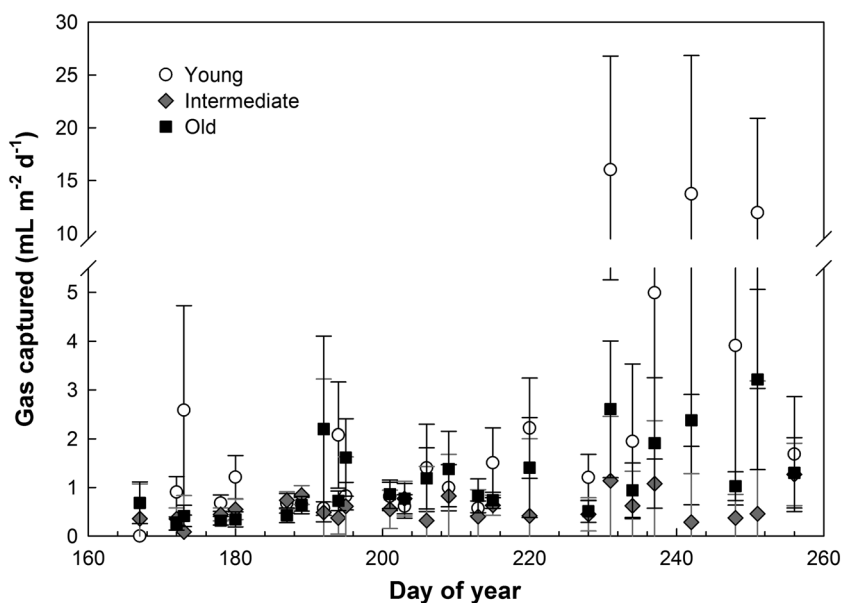
Figure 1. Daily bubble accumulation during the 2011 growing season at each collapse site. Open circles are young collapse, gray triangles are intermediate collapse, and black squares are old collapse site. Data are means ± 1 SE. Note the break in the y axis.

this bomb ^{14}C tracer into terrestrial C pools can be used to infer (1) the mean age of bulk C within the last 50–60 years at high (about 1 year) resolution, (2) the time since pools received inputs of plant biomass (atmospheric CO_2), or (3) the mixing of modern C from plant biomass with older C from a deeper source. We report ^{14}C data as isotope fractionation corrected $\Delta^{14}C$ [*Stuiver and Polach*, 1977], with the 1950 natural reference level being 0‰ by convention. If the $\Delta^{14}C$ value is positive (also known as modern), the majority of C has been fixed since 1950 with the bomb ^{14}C signature. If the $\Delta^{14}C$ value is negative, the bulk of the C was fixed before 1950 and has been in the soils undergoing radioactive decay for a longer time. We collected bubbles during peak biomass (8 August 2011) and just before surface soil freezeup (8 September 2011). During each campaign, bubbles were collected from six 20 cm bubble traps (three in the young collapse and three in the old collapse). Bubbles were injected into evacuated 30 mL glass serum vials sealed with butyl rubber stoppers (Bellco Glass, Vineland, NJ, USA) and crimp seals, similar to the collection method used by *Chanton et al.* [2008].

From the bubble sample, CH_4 and CO_2 were extracted in sequence using a continuous flow method *M. A. Pack et al.* (manuscript in preparation, 2014). Briefly, sample gas was injected into a C-free carrier gas stream (ultra zero air), CO_2 (and CO, which is not analyzed further) is frozen out of the gas stream, CH_4 is combusted to CO_2 in the presence of CuO at 975°C, and CH_4-derived and CO_2-derived CO_2 are subsequently purified, quantified, and graphitized using a sealed tube Zn reduction method [*Xu et al.*, 2007]. The graphite powder was analyzed for its ^{14}C content at the W. M. Keck carbon cycle accelerator mass spectrometry (AMS) laboratory of the University of California, Irvine. For graphite of >0.1 mgC, the precision is about ±2‰ (1 sigma) for modern samples and about ±15 ^{14}C years for samples up to ~5000 years old. A split of the purified CH_4-derived and CO_2-derived CO_2 was analyzed for its $\delta^{13}C$ signature on a Thermo Electron Gas Bench II coupled with a Finnigan Delta Plus isotope ratio mass spectrometer.

Mixtures of pre-bomb and post-bomb sources are likely, and therefore, we used ^{14}C isotope data and the U.S. Environmental Protection Agency isotope-mixing model (IsoSource version 1.3.1) [*Phillips and Gregg*, 2003] to explore the source of C contained in bubbles. In particular, we were interested in the relative contribution of thawed permafrost peat (i.e., peat previously frozen in permafrost) versus collapse bog peat (i.e., peat that accumulated after permafrost had thawed in our sites and this includes recent photosynthates) as sources of bubble CH_4 and CO_2. In IsoSource, we used three sources of bubble C: (1) modern (2011) plant inputs—assumed to be equivalent to atmospheric $\Delta^{14}C$ signatures (36‰ for both sites in 2011), (2) collapse scar peat inputs—assumed to represent $\Delta^{14}C$ signatures ranging from the timing of permafrost degradation in each

Table 1. CH_4 Concentration, Total Bubble Accumulation, and Ebullition Measured at Each Site in 2011[a]

Site (No. of Bubble Traps)	Mean CH_4 Content (%)	Median CH_4 Content (%)	Mean Total Bubbles (L m^{-2})	Median Total Bubbles (L m^{-2})	Mean Ebullition (mg CH_4 m^{-2} d^{-1})	Median Ebullition (mg CH_4 m^{-2} d^{-1})
Young collapse (10)	21.4 ± 2.7	20.3	8.5 ± 4.7	3.3	14.5 ± 5.68	5.7
Intermediate collapse (7)	23.0 ± 2.1	23.0	1.6 ± 2.2	1.6	3.0 ± 0.34	2.9
Old collapse (8)	25.6 ± 1.6	26.4	3.0 ± 0.9	1.9	6.3 ± 1.20	4.1

[a]Data are expressed both as means (±1 standard error) and medians.

site (see section 2) to 2011 (-11 and -22‰ for young and old collapse, respectively), and (3) thawed permafrost soil inputs—assumed to represent $\Delta^{14}C$ signatures ranging from the timing of basal peat initiation to the timing of permafrost degradation, thus reflecting $\Delta^{14}C$ signatures for when the system was a permafrost peatland (-287 and -279‰ for young and old collapse, respectively). The $\Delta^{14}C$ signatures were calculated based on site thaw history (see section 2). Because the latter two sources represent soil C pools with a combination of ages, we calculated the median age estimate for each source corresponding to when 50% of the peat stock had accumulated in each C pool based on a peat accumulation curve [*O'Donnell et al.*, 2012] and basal peat ages [*Jones et al.*, 2012] from similar collapse scar bog sites in interior Alaska.

3.4. Statistical Analyses

All analyses were performed in R version 2.14.1 (R Development Core Team 2011) at 95% confidence ($\alpha = 0.05$). We used both parametric and nonparametric one-way analysis of variance (Kruskal-Wallis) and subsequent post-hoc Tukey and Bonferroni tests to explore the effects of site on seasonal bubble capture (mL m^{-2} season^{-1}) and associated CH_4 flux (mg CH_4 m^{-2} season^{-1}) from the 20 and 60 cm bubble traps. Similar analyses were used to analyze the effects of site on vegetation, peat strength, and environmental variables. Nonparametric statistics were used when normal distributions of residuals could not be achieved. To ensure that the uneven sample size between the 20 cm ($n = 25$) and 60 cm ($n = 6$) bubble traps was not influencing our results, we resampled the 20 cm trap seasonal bubble capture data 5000 times randomly and ran a Mann-Whitney boot strap analysis on each subpopulation of 20 cm traps ($n = 6$) and the 60 cm traps ($n = 6$).

To explore controls on ebullition, we used linear mixed effects models with bottom-up Akaike information criterion model selection. The response variable was daily bubble rate (mL m^{-2} d^{-1}), and predictor variables included 5 cm soil temperature, VMC, depth to seasonal ice, as well as minimum and maximum atmospheric pressure between ebullition samplings and the change in minimum pressure between the day prior to sampling and sampling date. Bubble trap ID was used as a repeated measure. The pseudo-R-square for each best fitted model was calculated using a comparison of the original data and the predicted values. We used simple linear regression models to determine how much of the total monthly ebullition (mL m^{-2} month^{-1}) could be
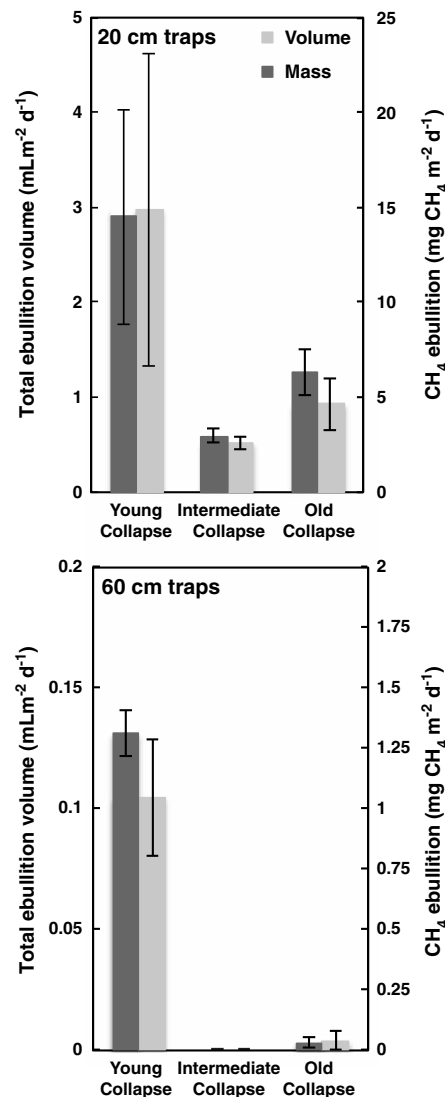

Figure 2. Ebullition measured in 20 and 60 cm bubble traps at the three collapse sites. Light gray bars are the volumetric ebullition, and dark gray bars are the mass ebullition in terms of CH_4. Data are means ± 1 SE. Note the differently scaled y axis.
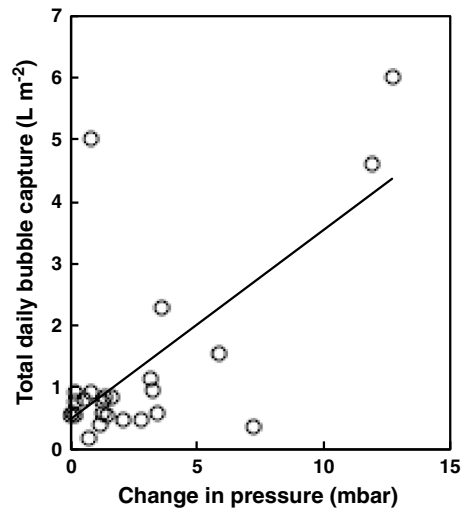
Figure 3. Relationship between the additive daily bubble capture across all total traps in three collapse bogs and the change in atmospheric pressure between the sampling day and 1 day prior ($y = 0.31$, $x + 0.5$, $R^2 = 0.45$, $F_{(1, 23)} = 19.04$, $p < 0.001$).

independently explained by mean monthly 5 cm soil temperature, VMC, and seasonal ice depth across sites.

We defined ebullition hot spots as bubble traps that exceeded the 75th percentile for total seasonal bubble accumulation, which was equivalent to bubble traps that accumulated more than 111.1 mL of gas over the 90 day sampling season. This led to the identification of six hot spots, two of which were located in the old collapse and four of which were located in the young collapse. To further explore the nature of ebullition, we divided daily bubble rates into steady versus episodic ebullition events. Episodic events were defined as bubble rates ≥0.9 mL/d (corresponding to the 75th percentile for daily bubble rates across sites). We tested for a negative correlation between the amount of episodic versus steady state ebullition at each trap expressed as a percentage of total bubble volume, which would suggest a trade-off between episodic and steady state ebullition. For both episodic and steady ebullition, we used linear regression models to explore relationships with sedge stem density and distance to the permafrost-thermokarst boundary.

4. Results

4.1. Ebullition and CH_4 Emission Across the Collapse Bogs

Bubble rates varied among sites and tended to be higher in the young collapse than the other sites (Figure 1). Across sites, more ebullition occurred in August than in June or July. The total cumulative bubble capture was 16.0 L m^{-2}, 19.1 L m^{-2}, and 83.5 L m^{-2} in June, July, and August, respectively. Sites had comparable mean and median CH_4 concentrations in bubbles (between 20.3 and 26.4% CH_4) ($F_{(2, 44)} = 0.92$, $p = 0.405$; Table 1). Concentrations of CO_2 in bubbles however were less than 4%. There were no significant differences in peat strength between the sites ($p > 0.1$).

Ebullition was greater by an order of magnitude in the 20 cm traps than in the 60 cm traps ($H_{(1)} = 14.07$, $p < 0.001$; Figure 2). Methane emission from the 20 cm traps averaged 8.65 ± 3.32 mg CH_4 m^{-2} d^{-1}, while emission from the 60 cm traps averaged 0.45 ± 0.28 mg CH_4 m^{-2} d^{-1} (Figure 2). Bootstrap analyses confirmed
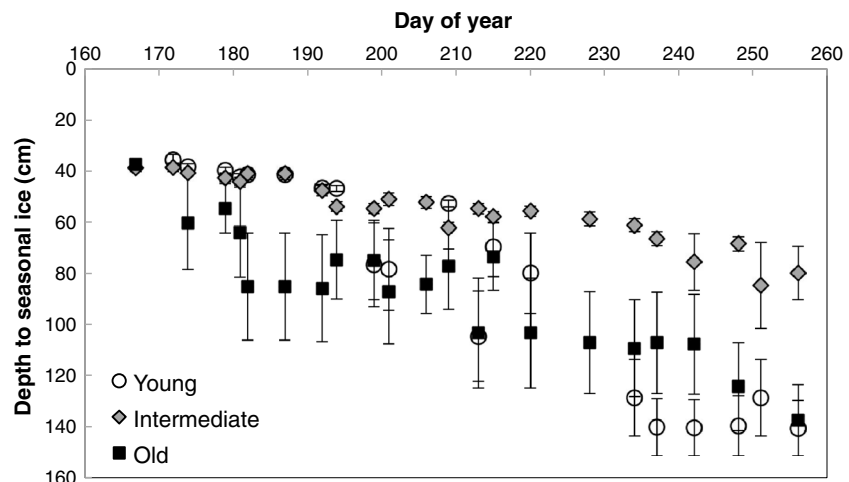

Figure 4. Depth of seasonal ice thaw (mean ± SE) at each collapse bog over the 90 day sampling period in 2011. Open circles are young collapse, gray triangles are intermediate collapse, and black squares are old collapse site data means ± 1 SE.

Table 2. Collapse Bog Environmental, Vegetation Stem Density Cover, and Peat Characteristics (Seasonal Means ± SE)

Parameter	Young Collapse	Intermediate Collapse	Old Collapse
Moisture (%VMC)	87 ± 2.9	67 ± 2.7	74 ± 2.4
Soil temperature (°C)	11.5 ± 0.2	9.6 ± 0.2	14.2 ± 0.4
Seasonal ice depth (cm)	80.6 ± 9.2	55.5 ± 2.7	87.7 ± 5.2
Seasonal ice thickness (cm)	na[a]	40.8 ± 6.04	15.5 ± 6.21
C. aquatilis stem density (stems/m^2)	204 ± 66	143 ± 40	76 ± 22
Sedge stem density (stems/m^2)	541 ± 96	538 ± 85	604 ± 84
Shrub stem density (stems/m^2)	52 ± 28	153 ± 53	164 ± 48
Fine root densty (mg/cm^3)	2.93 ± 0.40	1.68 ± 0.41	1.45 ± 0.43
Coarse root density (mg/cm^3)	na[a]	2.77 ± 2.06	0.09 ± 0.09
Bulk density (g/cm^3)	0.02 ± 0.01	0.12 ± 0.04	0.07 ± 0.01
Peat strength index (hits/cm)	0.69 ± 0.12	0.52 ± 0.07	0.20 ± 0.01

[a]na = data not available.

that the difference between the 20 and 60 cm traps was not driven by unequal sample sizes (all p's < 0.001). Unlike bubble production from the 20 cm traps, which was higher in the young collapse than in the other sites (Table 1), there were no differences among sites in bubble rates from the 60 cm traps ($H_{(2)}$ = 4.19, p = 0.123; Figure 2). The remainder of our results focus on the 20 cm bubble trap data.

Daily bubble rates in the 20 cm traps were regulated by an interaction between atmospheric pressure (Figure 3) and depth to seasonal ice. A model including absolute changes in atmospheric pressure, depth to seasonal ice, and the interaction between these effects explained 57% of the variation in daily bubble rates summed across traps at all three sites. The interaction means that the influence of atmospheric pressure on ebullition was not consistent throughout the season. Absence of seasonal ice later in the season (Figure 4) resulted in higher daily bubble rates with changes in pressure compared to the same pressure changes earlier in the season when seasonal ice was present. Interestingly, the addition of temperature to this model did not increase the model significance or strength and was not a significant predictor of daily bubble rates.

Controls on monthly total bubble rates (mL m^{-2} month^{-1}) also varied through the season, with monthly mean soil moisture, temperature, and depth to seasonal ice varying among the three sites (Table 2). Early in the growing season, soil moisture was the most important, although not significant, predictor of monthly total bubble rates (June to July moisture: R^2 = 0.12, $F_{(1,23)}$ = 3.037, p = 0.095), and soil temperature and depth to seasonal ice were weaker predictors of monthly total bubble rates (June to July temperature: R^2 = 0.005, $F_{(1, 23)}$ = 0.118, p = 0.734; June to July ice: R^2 = 0.02, $F_{(1, 23)}$ = 0.573, p = 0.457). Depth to seasonal ice became a significant predictor of monthly total bubble accumulation later in the growing season (August to September ice: R^2 = 0.22, $F_{(1, 23)}$ = 6.533, p = 0.018); increases in depth to seasonal ice related to seasonality (Figure 4).
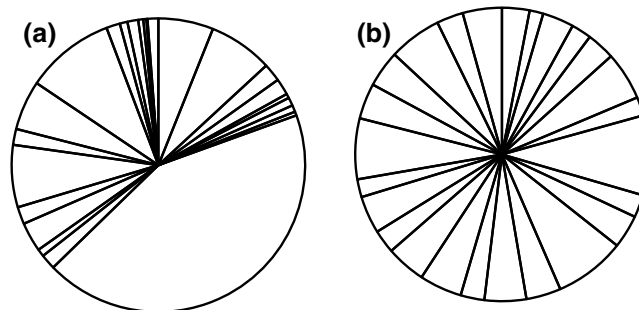

Figure 5. The contribution of each individual bubble trap to the total seasonal documented (a) episodic and (b) steady state ebullition; each trap is represented as a pie wedge.

Four traps in the young collapse and two traps in the old collapse were identified as hot spots. No traps in the intermediate collapse were identified as hot spots. Although there were no significant vegetation differences between traps identified as hot spots versus non-hot spots, the traps identified as hot spots tended to have higher sedge density and lower shrub densities than the other traps (hot spot traps: 607 ± 154 stems m^{-2}, n = 6; other traps: 580 ± 62 stems m^{-2}, n = 19). Traps identified as hot spots were located at similar distances to the
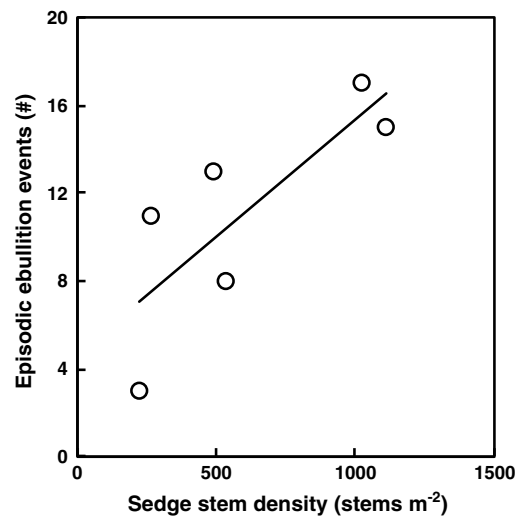
Figure 6. Relationship between the total sedge stem densities (stems per square meter of *C. aquatilis, E. chamissonis,* and *E. palustris*) and the number of episodic ebullition events from hot spots within three collapse bogs ($R^2 = 0.63$, $F_{(1, 4)} = 6.72$, $p = 0.06$).

permafrost-thermokarst boundary as the other traps ($p = 0.106$), although hot spot traps on average were situated 469 ± 143 cm from the permafrost-thermokarst boundary ($n = 6$), while the other traps were situated 332 ± 41 cm from the permafrost-thermokarst boundary ($n = 19$).

Episodic ebullition events, defined as events exceeding the 75th percentile of daily bubble rates from the 20 cm traps, accounted for 87% of total seasonal bubble capture across sites. Episodic ebullition events were spatially asynchronous and were dominated by just a few traps (Figure 5). Steady state ebullition events were defined as daily bubble rates below the 75th percentile and accounted for 13% of total seasonal bubble capture across sites. Steady state ebullition events were more spatially homogenized/equal among bubble traps (Figure 5). There was a negative correlation between episodic and steady state ebullition events ($P = -0.85$, $t_{(23)} = -7.63$, $p < 0.001$). Neither episodic ($p = 0.510$)

Table 3. Isotope Composition of Bubble CH_4 and CO_2 and Mean, Minimum, and Maximum Thawed Permafrost (Old) C Contributions in Percent to Bubbles Collected in August and September at the Old and Young Collapse Sites[a]

Collapse Site	Carbon Species	$\delta^{13}C$	University of California-Irvine AMS No.	$\Delta^{14}C$	Mean Old Carbon	Minimum Old Carbon	Maximum Old Carbon
		(‰)		(‰)	(%)	(%)	(%)
August	CO_2	−9.3	97,497	31.8	0.5	0	1
Old		−13.1	97,498	78.6	<0.1	0	<0.1
		−7.5	97,499	72.9	<0.1	0	<0.1
	CH_4	−51.3	97,483	102.6	<0.1	0	<0.1
		−52.4	97,484	111.7	<0.1	0	<0.1
		−52.9	97,486	101.4	<0.1	0	<0.1
Young	CO_2	−12.1	97,494	27.9	1.4	0	3
		−13.8	97,495	24.2	1.4	0	3
		−9.9	97,496	5.5	4.6	0	9
	CH_4	−54.5	97,480	53.2	<0.1	0	<0.1
		−54.0	97,481	51.3	<0.1	0	<0.1
		−55.4	97,482	48.7	<0.1	0	<0.1
September	CO_2	−9.9	107,313	21.7	1.9	0	4
Old		−12.8	107,315	29.8	0.8	0	2
		na[b]	107,316	38.8	<0.1	0	<0.1
	CH_4	−54.7	107,144	26.0	1.5	0	3
		−47.9	107,164	119.2	<0.1	0	<0.1
		−48.9	107,309	123.9	<0.1	0	<0.1
Young	CO_2	−12.5	107,317	29.9	0.8	0	2
		na[b]	107,318	−99.4	36.9	32	42
		na[b]	107,319	−9.7	7.0	0	14
	CH_4	−62.1	107,310	−35.8	15.6	9	22
		−50.1	107,311	49.9	<0.1	0	<0.1
		−52.0	107,312	67.8	<0.1	0	<0.1

[a]Values denoted as less than 0.1% did not conform to the isotope-mixing model parameters and are assumed to be negligible.
[b]na = data not available.

nor steady ebullition ($p = 0.847$) events were affected by sedge density or distance to the permafrost-thermokarst boundary ($p > 0.05$). We further examined controls on episodic ebullition events from the hot spot traps only. While this yielded a stronger relationship with sedge stem density, it was not significant ($p = 0.061$) likely due to small sample size (Figure 6). There was no relationship between episodic ebullition events from hot spot traps and distance to the permafrost-thermokarst boundary ($p = 0.656$).

4.2. Isotopic Composition of CH_4 and CO_2 in Bubbles

Young collapse bubbles consistently had more depleted $\Delta^{14}C$-CH_4 signatures than the old collapse bubbles, which could indicate contributions from pre-1950 (Table 3). In both sites, bubbles later in the season have more variable $\Delta^{14}C$-CH_4 signatures than earlier in the season. At peak biomass, $\Delta^{14}C$-CH_4 ranged from 48.7 to 53.2‰ at the young collapse and 101.4 to 111.7‰ at the old collapse. During the late season campaign, $\Delta^{14}C$-CH_4 ranged from -35.8 to 67.8‰ and 26.0 to 123.9‰ for the young and old collapse, respectively. The ^{14}C content of CO_2 showed similar trends but was more depleted (Table 3). The average $\delta^{13}C$ value of CH_4 was -53 ± 3.7‰, and the average $\delta^{13}C$ value of CO_2 was -11 ± 2.1‰ with more variation in September than August (Table 3).

The source of C in bubbles was interpreted to be predominately modern and was likely fixed after the midcentury bomb spike [*Levin et al.*, 2010]. Using the IsoSource model, we determined that the contribution of thawed permafrost soils to bubble C varied greatly between sites and sampling campaigns (Table 3). The young collapse site had thawed permafrost soil C contributions ranging from 0 to 42% and 0 to 22% for the CO_2 and CH_4, respectively, while the old collapse had thawed permafrost soil C contributions ranging from 0 to 4% and 0 to 3% for CO_2 and CH_4, respectively. Average contributions of permafrost C to bubble CH_4 were always less than 10% regardless of site and month (Table 3). We could not confidently partition the nonpermafrost C contribution into plant or collapse scar peat sources because the isotope-mixing model had many potential outcomes for these two sources. This challenge was due to the way in which we defined the collapse scar peat. However, we feel it is reasonable to assume that plant C was most likely impacting and controlling the CH_4 signatures and was definitely more important to bubble C than permafrost C.

5. Discussion

5.1. Spatial and Temporal Heterogeneity in Ebullition

Our results suggest that ebullition was greater in the young collapse site than in the old collapse site. The young collapse also had twice as many bubble traps designated as hot spots relative to the old collapse. More recently, thawed sites may support higher ebullition through a variety of mechanisms, including inputs of labile soil C inputs, the presence of plant communities or environmental conditions (i.e., warm and wet soils) that stimulate bubble production, or changes in peat properties that alter bubble storage and release.

Across all three of our sites, our measurement of bubble accumulation was dominated by episodic ebullition events, which accounted for ~87% of the total seasonal bubble capture. This is in contrast to the findings in temperate peatlands, where episodic ebullition contributed less to the total CH_4 flux than steady state ebullition [*Green and Baird*, 2013]. At our sites, few bubble traps contributed to episodic ebullition (hot spots); most of the traps in our measurement network were not associated with any episodic events. This fits with the definition of hot spots as "heterogeneous areas that have disproportionately high reaction rates compared to the surrounding region" [*McClain et al.*, 2003].

Across bubble traps, we found a negative relationship between episodic and steady state total seasonal ebullition. This relationship likely represents a trade-off, where an individual location is associated with either high bubble production through steady state ebullition or episodic ebullition but not both. Similar to our ebullition trade-off results but on an interseasonal time scale, *Mastepanov et al.* [2013] found that fall freezing in the tundra resulted in pulses of CH_4 that were subsequently associated with lower spring fluxes because the CH_4 pool was depleted over winter. Our results showed a negative relationship between ebullition processes within a season. Episodic ebullition may occur where confining layers in peat trap small subsurface bubbles and cause them to coalesce into larger bubbles before emission, which would also reduce bubble release as a steady state process [*Coulthard et al.*, 2009].

The effect of plant presence on ebullition has been predicted to be negative, because vascular plants serve as conduits for CH_4 release from pore water [*Chanton*, 2005; *Strack et al.*, 2006]. This was reaffirmed in a recent

study, showing that the presence of sedges resulted in higher total CH_4 emissions captured in static chambers but had no influence on episodic ebullition events [*Green and Baird*, 2011]. Our results do not indicate a negative effect of sedge cover on ebullition. Instead, we found a nonsignificant but compelling positive trend between sedge density and total seasonal bubble capture ($p = 0.06$ with $n = 6$). However, sedge density was confounded with distance from the thermokarst-permafrost boundary, as sedges were denser closer to the thaw margins. While sedge density was a stronger predictor of hot spot ebullition rates than distance to the thermokarst-permafrost boundary, we were not able to disentangle these two effects as controls on ebullition.

5.2. The Source of Bubble C

Shallow peat layers are associated with inputs of labile C substrates recently fixed from the atmosphere by plants, relatively warm temperatures, and dynamic water tables, all of which could stimulate bubble production [*Blodau*, 2002; *Kellner et al.*, 2006; *Coulthard et al.*, 2009]. On the other hand, deep peat layers were identified as the main source of ebullition in Minnesota temperate peatlands [*Glaser et al.*, 2004]. At our sites, three lines of evidence support the hypothesis that bubble production and CH_4 release associated with ebullition occur in surface peat layers more so than from depth. First, our 20 cm bubble traps accumulated on average 20 times more bubbles than the 60 cm bubble traps, suggesting that near-surface peat layers were a more important zone of bubble production than deeper peat across all of our sites. These findings are similar to patterns of ebullition in a temperate-rich fen, where more ebullition was captured in traps installed in shallow peat relative to traps installed in deeper peat [*Coulthard et al.*, 2009]. Second, our ^{14}C analyses suggest that the majority (typically >90%) of C contained in bubbles was derived from collapse scar bog peat that accumulated after permafrost thawed and modern plant inputs. While older C from the thawed permafrost soils was detected in some of our samples, it represented a small fraction of bubble C. Third, our results suggest that the largest episodic ebullition events occurred in areas with dense sedges. This could occur if sedge root exudates promote methanogenesis and bubble production, although sedge roots could also influence bubble entrapment and storage in peat layers. Another recent study further implies that there is a stronger relationship between vegetation composition and CH_4 compared to temperature and CH_4 [*Ward et al.*, 2013] suggesting that more attention should be paid to vegetation communities in predictive models.

While our results support the importance of plants and near-surface peat C to ebullition, they also suggest that thawed permafrost soils do contribute to ebullition in collapse bogs, particularly later in the ice-free season. The 60 cm bubble traps captured a small amount of bubbles, primarily in the young collapse site. These traps only accumulated bubbles once the seasonal ice had thawed appreciably below 60 cm. This trend likely occurs because (1) warmer peat temperatures stimulate methanogenesis and bubble formation, (2) warmer conditions reduce the solubility of CH_4 in peat, and (3) thaw of seasonal ice promotes mineralization of deeper peat, allowing for upward diffusion and bubble movement from the previously capped talik zone compared to earlier in the growing season when seasonal ice is still present as a barrier between these two vertical zones.

Additionally, our ^{14}C analyses confirmed that some C derived from thawed permafrost soils was contained in bubbles. The young collapse site had larger maximum contributions of this permafrost soil C in bubbles than the old collapse site during both sampling campaigns. The young collapse had more variable and greater thawed permafrost soil C contribution ranges than the old collapse for both CH_4 and CO_2. CO_2 was always more depleted than the CH_4, which supports the idea that the majority of the CH_4 is derived from plant C sources and not CO_2. In northern mountain birch forests in Sweden, a priming effect of permafrost C by roots was observed [*Hartley et al.*, 2012], a mechanism that could also be at play in our sites during early post-thaw C loss. In both sites, the contribution of thawed permafrost soil C to bubbles was more prevalent later in the growing season. A ^{14}C partitioning study in Finnish peat also showed a seasonal trade-off between plant- and soil-derived C, with an increase in the soil-derived C signature later in the growing season [*Biasi et al.*, 2011]. In general, it makes sense that emission of C from thawed permafrost soils would peak late in the growing season, when seasonal ice has thawed leading to warmer peat at depth. Our measured proportions of $C-CO_2$ in bubbles attributed to thawed permafrost soil inputs are comparable to previous studies. For example, *Schuur et al.* [2009] found that on average, 8–16% of old C was released during ecosystem respiration in Alaskan thermokarst sites (although we note that these sites thawed more recently than our sites).

5.3. Implications for Representing Ebullition in Ecosystem Models

Our study highlights the relationships between ebullition and environmental predictors that may be useful for improving the representation of ebullition in C cycling and Earth system models. Large changes in atmospheric pressure can cause bubble volumes to change following the ideal gas law [*Waddington et al.*, 2009], stimulating release in peatlands [*Strack et al.*, 2005; *Tokida et al.*, 2007; *Comas et al.*, 2011; *Comas and Wright*, 2012]. While some studies have emphasized the importance of decreases in atmospheric pressure [*Strack et al.*, 2005; *Tokida et al.*, 2007], others have shown that increases in atmospheric pressure can cause ebullition events [*Comas et al.*, 2011; *Comas and Wright*, 2012]. Increases in atmospheric pressure will decrease bubble volume and could increase bubble mobility through peat pore spaces [*Beckwith and Baird*, 2001; *Rosenberry et al.*, 2006]. However, decreases in atmospheric pressure will cause bubble volumes to increase, and this may destabilize the structural stability of the bubble and release a cascade of smaller bubbles [*Coulthard et al.*, 2009]. Here we found a strong relationship between ebullition and absolute changes in atmospheric pressure that was consistent with both increases and decreases in atmospheric pressure. The strength of this relationship became stronger later in the growing season as seasonal ice thawed, suggesting that changes in atmospheric pressure were more effective at releasing bubbles without the physical barrier of seasonal ice. Alternatively, thaw of seasonal ice leads to warmer soils and exposes more peat to microbial activity and possible increased substrate availability, all of which would increase bubble production in peat. This could also lead to stronger relationships between atmospheric pressure and ebullition late in the growing season, although we note that temperature was not a significant predictor of ebullition in our study. Together, depth to seasonal ice and change in atmospheric pressure explained almost 60% of variation in daily bubble accumulation/production rates. We attempted to use peat strength as a nondestructive measure of bubble-confining layers. Although our results showed no relationship between peat strength and daily bubble accumulation rate, it seems likely that the distribution and number of layers in peat will control the degree of episodic ebullition in combination with changes in atmospheric pressure and available organic matter.

Our results highlight different controls on steady state versus episodic ebullition. While the current threshold approach [*Wania et al.*, 2010] and fuzzy threshold approach [*Kellner et al.*, 2006] may be suitable for modeling steady state ebullition, improved representation of episodic ebullition in models likely will require a term for entrapped gas storage. Buried confining layers, such as dense roots, may also trap small bubbles indefinitely. The input of small bubbles through methanogenesis may remain constant, possibly leading to steady state ebullition, or bubbles may collect and trigger an avalanching effect where bubbles "fall off the sand pile" and lead to episodic ebullition events. Our results provide empirical evidence of a trade-off between steady state and episodic ebullition and conceptual support for the "inverted sandpile" model [*Coulthard et al.*, 2009] and its prediction of bubble cascades in collapse bogs.

6. Conclusions

Our study investigated controls on ebullition in peatlands affected by permafrost thaw in interior Alaska. We found that the majority of bubbles came from surface peat layers. However, some bubbles were produced in deeper peat layers, and the thawed permafrost soil pool was attributed as a source for 7% and 1% of September bubble C-CH_4 on average in the young and old collapse sites, respectively. Together, our results support both of our main hypotheses and suggest that permafrost thaw increases CH_4 loss to the atmosphere by (1) producing anaerobic environments dominated by sedges that promote CH_4 production and (2) stimulating the mineralization of older C stored in the thawed permafrost soil pool. We also identified relationships between changes in atmospheric pressure and ebullition that were dependent on the presence of seasonal ice in our sites. Our research highlights the need for more sophisticated representation of ebullition within global C and Earth system models, which we believe is necessary for understanding present and future CH_4 fluxes at northern high latitudes.

References

Baird, A. J., C. W. Beckwith, S. Waldron, and J. M. Waddington (2004), Ebullition of methane-containing gas bubbles from near-surface *Sphagnum* peat, *Geophys. Res. Lett.*, 31, L21505, doi:10.1029/2004GL021157.
Beckwith, C. W., and A. J. Baird (2001), Effect of biogenic bubbles on water flow through poorly decomposed blanket peat, *Water Resour. Res.*, 37, 551–558, doi:10.1029/2000WR900303.

Beilman, D. W. (2001), Plant community and diversity change due to localized permafrost dynamics in bogs of western Canada, *Can. J. Bot.*, *79*, 983–993, doi:10.1139/b01-070.

Biasi, C., N. M. Tavi, S. Jokinen, N. Shurpali, K. Hamalainen, J. Jungner, M. Oinonen, and P. J. Martikainen (2011), Differentiating sources of CO_2 from organic soil under bioenergy crop cultivation: A field-based approach using ^{14}C, *Soil Biol. Biochem.*, *43*, 2406–2409, doi:10.1016/j. soilbio.2011.08.003.

Blodau, C. (2002), Carbon cycling in peatlands – A review of processes and controls, *Environ. Rev.*, *10*, 111–134, doi:10.1139/a02-004.

Chanton, J. P. (2005), The effect of gas transport on the isotope signature of methane in wetlands, *Org. Chem.*, *36*, 753–768, doi:10.1016/j. orggeochem.2004.10.007.

Chanton, J. P., and J. W. H. Dacey (1991), Effects of vegetation on methane flux, reservoirs, and carbon isotopic composition, in *Trace Gas Emissions by Plants*, edited by T. D. Sharkey, E. A. Holland, and H. A. Mooney, pp. 65–92, Academic, San Diego, California, USA.

Chanton, J. P., P. H. Glaser, L. S. Chasar, D. J. Burdige, M. E. Hines, D. I. Sigel, L. B. Tremblay, and W. T. Cooper (2008), Radiocarbon evidence for the importance of surface vegetation on fermentation and methanogenesis in contrasting types of boreal peatlands, *Global Biogeochem. Cycles*, *22*, GB4022, doi:10.1029/2008GB003274.

Comas, X., and W. Wright (2012), Heterogeneity of biogenic gas ebullition in subtropical peat soils is revealed using time-lapse cameras, *Water Resour. Res.*, *48*, W04601, doi:10.1029/2011WR011654.

Comas, X., L. Slater, and A. Reeve (2011), Atmospheric pressure drives changes in the vertical distribution of biogenic free-phase gasses in a northern peatland, *J. Geophys. Res.*, *116*, G04014, doi:10.1029/2011JG001701.

Coulthard, T. J., A. J. Baird, J. Ramirez, and J. M. Waddington (2009), Methane dynamics in peat: Importance of shallow peats and a novel reduced−complexity approach for modeling ebullition, in *Carbon Cycling in Northern Peatlands*, Geophysical Monograph Series 184, edited by A. J. Baird et al., pp. 173–185, AGU, Washington D. C.

Cronk, J. K., and M. S. Fennessy (2001), *Wetland Plants: Biology and Ecology*, CRC Press LLC, Boca Raton, FL, USA.

Glaser, P. H., J. P. Chanton, P. Morin, D. O. Rosenberry, D. I. Siegel, O. Ruud, L. I. Chasar, and A. S. Reeve (2004), Surface deformations as indicators of deep ebullition fluxes in a large northern peatland, *Global Biogeochem. Cycles*, *18*, GB1003, doi:10.1029/2003GB002069.

Green, S. M., and A. J. Baird (2011), A mesocosm study of the role of the sedge *Eriophorum angustifolium* in the efflux of methane—including that due to episodic ebullition—from peatlands, *Plant Soil*, doi:10.1007/s11104-011-0945-1.

Green, S. M., and A. J. Baird (2013), The importance of episodic ebullition methane losses from three peatland microhabitats: a controlled-environment study, *Eur. J. Soil Sci.*, *64*, 27–36, doi:10.1111/ejss.12015.

Harden, J. W., et al. (2012), Field information links permafrost carbon to physical vulnerabilities of thawing, *Geophys. Res. Lett.*, *39*, L15704, doi:10.1029/2012GL051958.

Hartley, I. P., M. H. Garnett, M. Sommerkorn, D. W. Hopkins, B. J. Fletcher, V. L. Sloan, G. K. Phoenix, and P. A. Wookey (2012), A potential loss of carbon associated with greater plant growth in the European Arctic, *Nat. Clim. Change*, *2*, 875–879, doi:10.1038/nclimate1575.

Hinzman, L. D., et al. (2005), Evidence and implications of recent climate change in northern Alaska and other Arctic regions, *Clim. Change*, *72*, 251–298, doi:10.1007/s10584-005-5352-2.

Hutchinson, G. (1957), *A Treatise on Limnology*, Geo. Phys. Chem., vol. 1, pp. 1015, John Wiley, Hoboken, N. J.

Intergovernmental Panel on Climate Change (2013), Climate Change 2013 – The Physical Science Basis. WGI AR5 Final Draft (version 7 June 2013).

Jones, M. C., R. K. Booth, Z. Yu, and P. Ferry (2012), A 2200-year record of permafrost dynamics and carbon cycling in a collapse-scar bog, interior Alaska, *Ecosystems*, doi:10.1007/s10021-012-9592-5.

Kasischke, E. S., L. L. Bourgeau-Chavez, A. R. Rober, K. H. Wyatt, J. M. Waddington, and M. R. Turetsky (2009), Effects of soil moisture and water depth on ERS SAE backscatter measurements from an Alaskan wetland complex, *Remote Sens. Environ.*, *113*, 1868–1873, doi:10.1016/j. res.2009.04.006.

Kellner, E., J. M. Waddington, and J. S. Price (2005), Dynamics of biogenic gas bubbles in peat: Potential effects on water storage and peat deformation, *Water Resour. Res.*, *41*, W08417, doi:10.1029/2004WR003732.

Kellner, E., A. J. Baird, M. Oosterwoud, K. Harrison, and J. M. Waddington (2006), Effect of temperature and atmospheric pressure on methane (CH_4) ebullition from near-surface peats, *Geophys. Res. Lett.*, *33*, L18405, doi:10.1029/2006GL027509.

King, J. Y., W. S. Reeburgh, and S. K. Regli (1998), Methane emission and transport by arctic sedges in Alaska: Results of a vegetation removal experiment, *J. Geophys. Res.*, *103*, 29,083–29,092, doi:10.1029/98JD00052.

Levin, I., T. Naegler, B. Kromer, M. Diehl, R. J. Francey, A. Gomez-Pelaez, L. P. Steele, D. Wagenbach, R. Weller, and D. E. Worthy (2010), Observations and modelling of the global distribution and long-term trend of atmospheric $^{14}CO_2$, *Tellus*, *62B*, 26–46, doi:10.1111/j.1600-0889.2009.00446.x.

Mastepanov, M., C. Sigsgaard, T. Tagesson, L. Strom, M. P. Tamstorf, M. Lund, and T. R. Christensen (2013), Revisiting factors controlling methane emissions from high-Arctic tundra, *Biogeosciences*, *10*, 5139–5158, doi:10.5194/bg-10-5139-2013.

McClain, M. E., et al. (2003), Biogeochemical hot spots and hot moments at the interface of terrestrial and aquatic ecosystems, *Ecosystems*, *6*, 301–312, doi:10.1007/s10021-003-0161-9.

O'Donnell, J. A., M. T. Jorgenson, J. W. Harden, A. D. McGuire, M. Z. Kanevskiy, and K. P. Wickland (2012), The effects of permafrost thaw on soil hydrologic, thermal, and carbon dynamics in an Alaskan peatland, *Ecosystems*, *15*, 213–229, doi:10.1007/s10021-011-9504-0.

Phillips, D. L., and J. W. Gregg (2003), Source partitioning using stable isotopes: coping with too many sources, *Oecologia*, *136*, 261–269, doi:10.1007/s00442-003-1218-3.

Prater, J. L., J. P. Chanton, and G. J. Whiting (2007), Variation in methane production pathways associated with permafrost decomposition in collapse scar bogs of Alberta, Canada, *Global Biogeochem. Cycles*, *21*, GB4004, doi:10.1029/2006GB002866.

Rosenberry, D. O., P. H. Glaser, D. I. Siegel, and E. P. Weeks (2003), Use of hydraulic head to estimate volumetric gas content and ebullition flux in northern peatlands, *Water Resour. Res.*, *39*(3), 1066, doi:10.1029/2002WR001377.

Rosenberry, D. O., P. H. Glaser, and D. I. Siegel (2006), The hydrology of northern peatlands as affected by biogenic gas: Current developments and research needs, *Hydrol. Processes*, *20*, 3601–3610, doi:10.1002/hyp.6377.

Schutz, H., and P. Schroder (1991), Role of plants in regulating the methane flux to the atmosphere, in *Trace Gas Emissions by Plants*, edited by E. H. Sharkey and H. Mooney, pp. 29–57, University Press, San Diego, California.

Schuur, E. A. G., J. G. Vogel, K. G. Crummer, H. Lee, J. O. Sickman, and T. E. Osterkamp (2009), The effect of permafrost thaw on old carbon release and net carbon exchange from tundra, *Nature*, *459*, 556–559, doi:10.1038/nature08031.

Shea, K. S. (2010), Physical and ecological controls on methane release from a boreal peatland. M.S. Thesis. Integrative Biology, University of Guelph, Guelph, Ontario, Canada.

Strack, M. E., E. Kellner, and J. M. Waddington (2005), Dynamics of biogenic gas bubbles and their effects on peatland biogeochemistry, *Global Biogeochem. Cycles*, *19*, GB1003, doi:10.1029/2004GB002330.

Strack, M. E., E. Kellner, and J. M. Waddington (2006), Effect of entrapped gas on peatland surface level fluctuations, *Hydrol. Processes*, *20*, 3611–3622, doi:10.1002/hyp.6518.

Stuiver, M., and H. A. Polach (1977), Discussion: Reporting of [14]C Data, *Radiocarbon*, *19*, 355–363.

Tokida, T., T. Miyazaki, M. Mizoguchi, O. Nagata, F. Takakai, A. Kagemoto, and R. Hatano (2007), Falling atmospheric pressure as a trigger for methane ebullition from peatland, *Global Biogeochem. Cycles*, *21*, GB2003, doi:10.1029/2006GB002790.

Trumbore, S. (2006), Carbon respired by terrestrial ecosystems – Recent progress and challenges, *Global Change Biol.*, *12*, 141–153, doi:10.1111/j.1365-2486.2006.01067.x.

Trumbore, S. (2009), Radiocarbon and soil carbon dynamics, *Annu. Rev. Earth Planet. Sci.*, *37*, 47–66, doi:10.1146/annurev.earth.36.031207.124300.

Turetsky, M. R., R. K. Wieder, and D. H. Vitt (2002), Boreal peatland C fluxes under varying permafrost regimes, *Soil Biol. Biochem.*, *34*, 907–912, doi:10.1016/S0038-0717(02)00022-6.

Waddington, J. M., K. Harrison, E. Kellner, and A. J. Baird (2009), Effect of atmospheric pressure and temperature on entrapped gas content in peat, *Hydrol. Processes*, *23*, 2970–2980, doi:10.1002/hyp.7412.

Waddington, J. M., E. Kellner, M. Strack, and J. S. Price (2010), Differential peat deformation, compressibility, and water storage between peatland microforms: Implications for ecosystem function and development, *Water Resour. Res.*, *46*, W07538, doi:10.1029/2009WR008802.

Wania, R., I. Ross, and I. C. Prentice (2010), Implementation and evaluation of a new methane model within a dynamic global vegetation model: LPJ-WHyMe v1.3.1, *Geosci. Model Dev.*, *3*, 565–584, doi:10.5194/gmdd-3-1-2010.

Ward, S. E., N. J. Ostle, S. Oakley, H. Quirk, P. A. Henrys, and R. D. Bardgett (2013), Warming effects on greenhouse gas fluxes in peatlands are modulated by vegetation composition, *Ecology Lett.*, *16*, 1285–1293, doi:10.1111/ele.12167.

Whalen, S. C. (2005), Biogeochemistry of methane exchange between natural wetlands and the atmosphere, *Environ. Eng. Sci.*, *22*, 73–94, doi:10.1089/ees.2005.22.73.

Wickland, K. P., R. G. Striegl, J. C. Neff, and T. Sachs (2006), Effects of permafrost melting on CO2 and CH4 exchange of a poorly drained black spruce lowland, *J. Geophys. Res.*, *111*, G02011, doi:10.1029/2005JG000099.

Xu, X., S. E. Trumbore, S. H. Zheng, J. R. Southon, K. E. McDuffee, M. Luttgen, and J. C. Liu (2007), Modifying a sealed tube zinc reduction method for preparation of AMS graphite targets: Reducing background and attaining high precision, *Nucl. Instrum. Methods Phys. Res. Section B*, *259*, 320–329, doi:10.1016/j.nimb.2007.01.175.